Journal of Composite Materials

Microscale damage mechanisms and degradation of fiber-reinforced composites for wind energy applications: results of Danish–Chinese collaborative investigations

L Mishnaevsky, Jr, HW Zhou, HY Yi, RD Peng, HW Wang, GM Dai, LL Gui and X Zhang

Microscale damage mechanisms and degradation of fiber-reinforced composites for wind energy applications: results of Danish–Chinese collaborative investigations

L Mishnaevsky Jr[1], HW Zhou[2], HY Yi[2], RD Peng[2], HW Wang[3], GM Dai[1], LL Gui[2] and X Zhang[2]

Abstract

Recent research works in the area of experimental and computational analyses of microscale mechanisms of strength, damage and degradation of glass fiber polymer composites for wind energy applications, which were carried out in the framework of a series of Sino–Danish collaborative research projects, are summarized in this article. In a series of scanning electron microscopy in situ experimental studies of composite degradation under off-axis tensile, compressive and cyclic loadings as well as three-dimensional computational experiments based on micromechanics of composites and damage mechanics, typical damage mechanisms of wind turbine blade composites were clarified. It was demonstrated that the damage mechanisms in the composites strongly depend on the orientation angle of the applied loading with the fiber direction. The matrix cracking was observed to be the main damage mechanism for tensile axial (or slightly off-axis axial) loading; for all other cases (off-axis tensile, compressive and cyclic tensile loadings), the interface debonding and shear control the damage mechanisms.

Keywords

Composites, wind blades, damage, compression

Introduction

The European Union (EU) has set a target to receive 20% of its energy needs from renewables by 2020. To achieve this goal, the offshore wind energy capacity of EU should be expanded by two orders of magnitude.

The expansion of wind energy production would require the installation and use of very large wind turbines (8–10 MW and higher) standing in wind farms of several hundred megawatts capacity. Generally, a wind turbine should work for 20–25 years without having to be repaired and with minimum maintenance.[1,2] The potential costs of maintenance, repair and replacement of damaged 100 m large wind turbines, standing offshore, can be huge and should be kept as low as possible.

In order to ensure the required reliability and lifetime of wind turbines, we should know and be able to control the damage mechanisms in wind turbine materials.

A rotor is the highest cost component of a wind turbine.[3] Blades represent the most important composite-based part of a wind turbine, whose properties quite often determine the performances and lifetime of the turbine. Several groups of Danish and Chinese scientists, from Technical University of Denmark, China University of Mining and Technology and Tianjin

[1]Department of Wind Energy, Technical University of Denmark, Denmark
[2]State Key Laboratory of Coal Resources and Safe Mining, China University of Mining and Technology, China
[3]School of Mechanical Engineering, Tianjin University of Commerce, China

Corresponding author:
L Mishnaevsky Jr, Department of Wind Energy, Technical University of Denmark, Risø Campus, DK-4000 Roskilde, Denmark.
Email: lemi@dtu.dk

University of Commerce, joined forces to investigate the mechanisms of damage and degradation of wind blade composites under various loadings. The goal of this series of experimental, theoretical and numerical investigations was to explore and analyze the damage mechanisms and degradation of composite materials used for blades of large wind turbines.

Wind turbine blades are subject to quite complex external loadings, which vary randomly both in value and direction. The loading on the blades includes the flapwise and edgewise bending loads, gravitational loads, inertia forces, loads due to pitch acceleration as well as torsional loading. While the flapwise load is caused mainly by the wind pressure, the edgewise load is caused both by gravitational forces and torque load. The highest edgewise bending moment is at the blade root.

The flapwise and edgewise bending loads cause high longitudinal, tensile and compressive stresses in the composite material. While the upwind side of the blades is subject to tensile stresses, the downwind side is subject to compression. According to Thomsen,[4] these two moments are responsible for 97% of the damage in blades. The wind blades are also subject to cyclic loadings caused by wind variations, turbulences, wind shear and other effects such as pressure variations of air around the tower.

Thus, when studying strength and damage mechanisms of composites, one should pay special attention to off-axis, multiaxial, compressive and shear loadings of the unidirectional composites. The goal of this research work is to study the damage mechanisms of glass fiber-reinforced polymer (GFRP) composites under off-axis, cyclic and compressive loadings, using both experimental and numerical approaches.

Micromechanism of damage growth and degradation of GFRP composites: experimental investigations

Scanning electron microscopy in situ experiments: testing machine and materials

In order to clarify the effect of the loading direction on the strength of wind blade materials, scanning electron microscopy (SEM) (Figure 1) in situ experimental investigations of damage growth in composites under different loading conditions have been carried out.

The testing system, SEM-servopulser, was developed and provided by Shimadzu Co., and is available at China University of Mining and Technology (Beijing). The system is used for a real-time in situ observation of the meso- and microscale structural changes and the flaw evolution of the metal and nonmetal materials that are subjected to static or dynamic loads. The system is controlled by the full digital servo hydraulic control and allows loading up to $\pm 10\,$KN, load frequency: 0.00001–$10\,$Hz (which may be extended to $100\,$Hz if one uses very small stroke range), and temperature can range from room temperature up to $800°$C. Different loading modes can be employed: tensile, compression and three-point bending. Other parameters are as follows: magnification, 35–$200,000\times$; scanning speed, 0.27–$9.6\,$s/f; observation resolution, $5.5\,$nm (low vacuum) and $3.5\,$nm (high vacuum).
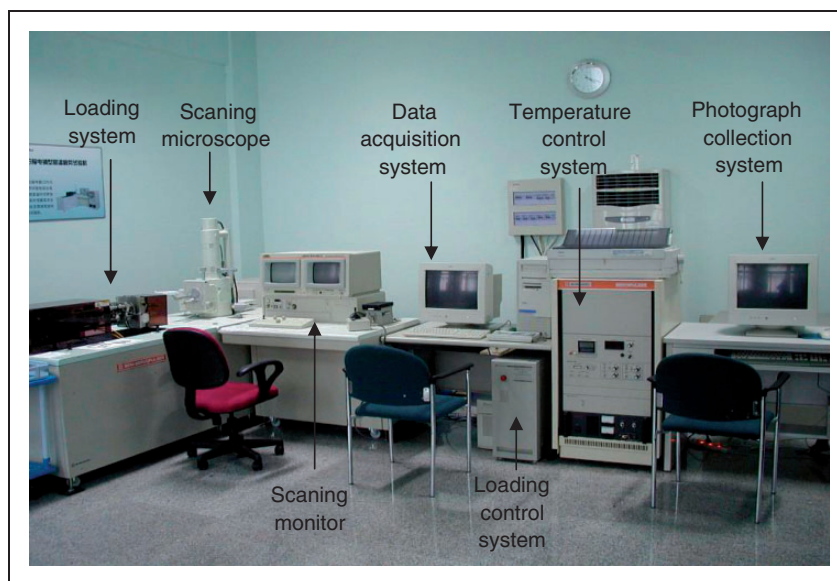

Figure 1. High temperature fatigue testing system with scanning electron microscopy.

The samples produced from GFRP were provided by the Knowledge Centre of Wind Turbine Materials and Constructions, the Netherlands. The specifications of these materials are as follows: identification number 595/c, system resin RIM 135, system hardener RIM/H 134/137, system mix ratio 100/30, vacuum curing 1000, post-cure 10 h at 70°C, Saertex weaver, curing tabs glue 2 h at 65°C.

First, the specimens for three-point bending and uniaxial tensile, compressive and tension–tension cyclic loading tests, with fibers volume fraction of 27.5%, were cut using water jet technology into needed shape and size and then the surfaces for observation in SEM was sand-polished. The specimens were put into an ultrasonic cleaning machine for 3–5 min to wash away the dust using pure alcohol. In addition, a hydronium sputtering instrument (type: KYKY SBC-12) was employed to gild the specimen for 200 s to obtain secondary electrons, thereby improving the quality of the real-time observations.

In order to investigate the influence of fiber orientation angles on the mechanical behavior of composite materials, the fibers were arranged at different orientation angles with respect to horizontal direction such as 0°, 15°, 30°, 45°, 60°, 75° and 90°. Three specimens were prepared for each orientation angle.

Three-point bending tests

A series of three-point bending tests has been carried out to characterize the effect of the off-axis loading on the damage in composites (also, specimens with notches). The specimens were fixed on the platform of the loading system (Figure 1) for three-point bending test, which was then inserted into the SEM chamber. The prefabricated notch in the specimens should be placed right under the loading bar (Figure 2(a)). Vacuum was created so that the surface image of the sample could be captured clearly. A displacement-controlled load was applied to the samples with loading rate of 1.5×10^{-3} mm/s until the sample fails. During the loading, displacements (i.e. the deflection of a specimen) and loads were recorded automatically by the test system. The test was stopped when load decreased to a very small level after the peak load.

By summarizing the experimental results of the three groups of samples with different orientation angles of fibers, the dependence of the mechanical parameters on the orientation angles of fibers was analyzed.[5] The regression analysis showed that the peak strengths, the elastic strengths and the elastic modulus of the composites decease almost linearly with the orientation angles of fibers (Figure 2(b)).

Tensile tests

Furthermore, a series of tensile deformation tests have been carried out. GFRP composite specimens (Figure 3) were subject to tensile loading under SEM in situ observations. Figure 4 shows the stress–strain curves of the composites, with corresponding micrographs. Again, it was observed that while the main mechanism of degradation of the composite is matrix cracking caused by high normal stresses for zero or very low angles between fibers and loading vectors, the mechanisms of degradation of the composites switch at high angles, to the shear stress-controlled interface debonding.

In Figure 4(a) (axial tensile loading), cracks were initiated at point 2 of the load-deflection curve. At point 3, a crack initiated away from the notched area and propagated vertically along the fibers. Thus, the load–deflection curve went down slowly. The matrix cracked apparently due to the tensile stresses. At point 5 and further onward, the curve remained at a constant certain level. Although there was a crack at the end of the specimen, obviously, fibers remained intact. In Figure 4(b) and (c), the crack initiated at point 2 (Figure 4(b)) and point 3 (Figure 4(c)) of the stress–strain curves. Then, the cracks propagated along the fibers. Correspondingly, the curves dropped quickly and the specimens failed. From the micrographs, corresponding to point 3 in Figure 4(b) and point 4 in Figure 4(c), one can see that the cracks tend to propagate over fibers.

In the case of the specimen with fiber orientation of 45° (Figure 4(d)), at point 2, a small delimitation was observed, leading to a downward jump of the load–deflection curves. Since the load–deflection curve went up again, one can see that it did not lead to failure. At point 4, shear cracks initiated and propagated along the 45° direction and the load–deflection curve moved downward again. Thus, the specimen with fiber orientation of 45° failed mainly because of shear crack formation. For the specimen with fiber orientation of 90° (Figure 4(e)), when the deformation reached point 3, the matrix cracked and load dropped immediately, while fibers remained intact. From point 3 onwards, fibers could bear the load up to point 5; then the fibers cracked and that led to full specimen failure.

Compression loading

In the further series of tests, we studied the compressive damage mechanisms of the composites. Figure 5 shows
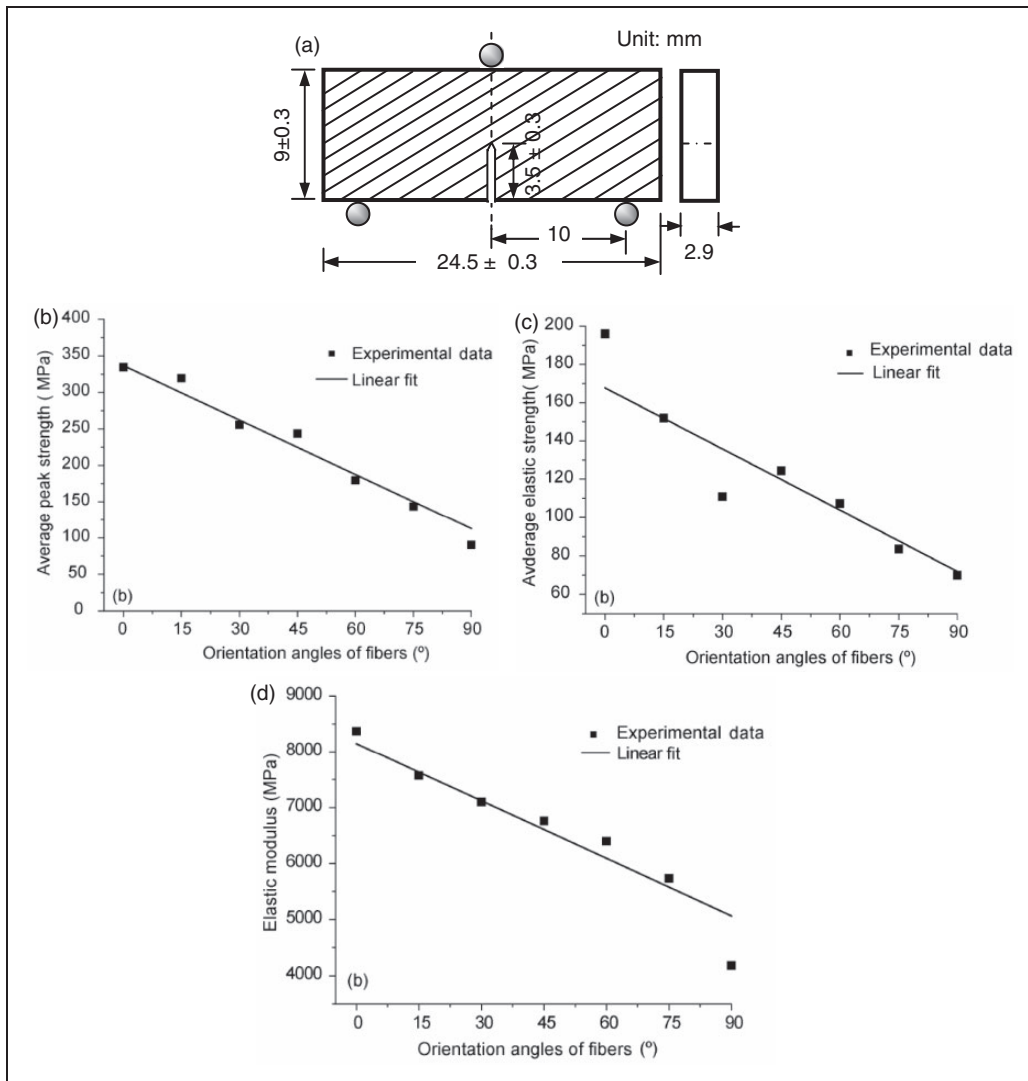
Figure 2. (a) Dimensions of three-point bending specimen and the effect of the fiber orientation on the mechanical properties of the composites: (b) average peak strength, (c) average elastic strength and (d) elastic modulus.
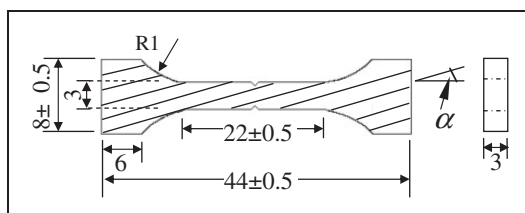

Figure 3. Dimensions of specimens for tensile tests (mm).

the dimension of specimen for compression test and the appearance of cracks after failure of the composite and Figure 6 shows the peak stress plotted versus the fiber/ loading angle. The strength of the composite decreases with increasing the angles at first and slightly increases after the angle reaches 45° (Figure 6).

In the tests, it was observed that the main damage mechanism under compression was the fiber buckling and kinking at the end of sample at smaller angles and shear or delamination at large angles between fibers and the loading direction (Figure 5). One can see the kinked fibers and growing cracks in Figure 5(b) (axial loading) and the kink bands and, again, growing debonding cracks in Figure 5(c)–(e) (angles 15°, 30° and 60°). An interesting crack, with bridging fibers and matrix regions, and branched crack path can be seen in Figure 5(g) (90°). Apparently, the complexity of stress state and mode II and II components of fracture mechanisms increase with increasing the angle between the fibers and loading vector, thus leading to the complex interactions of kinked fibers, interface debonding and growing cracks.
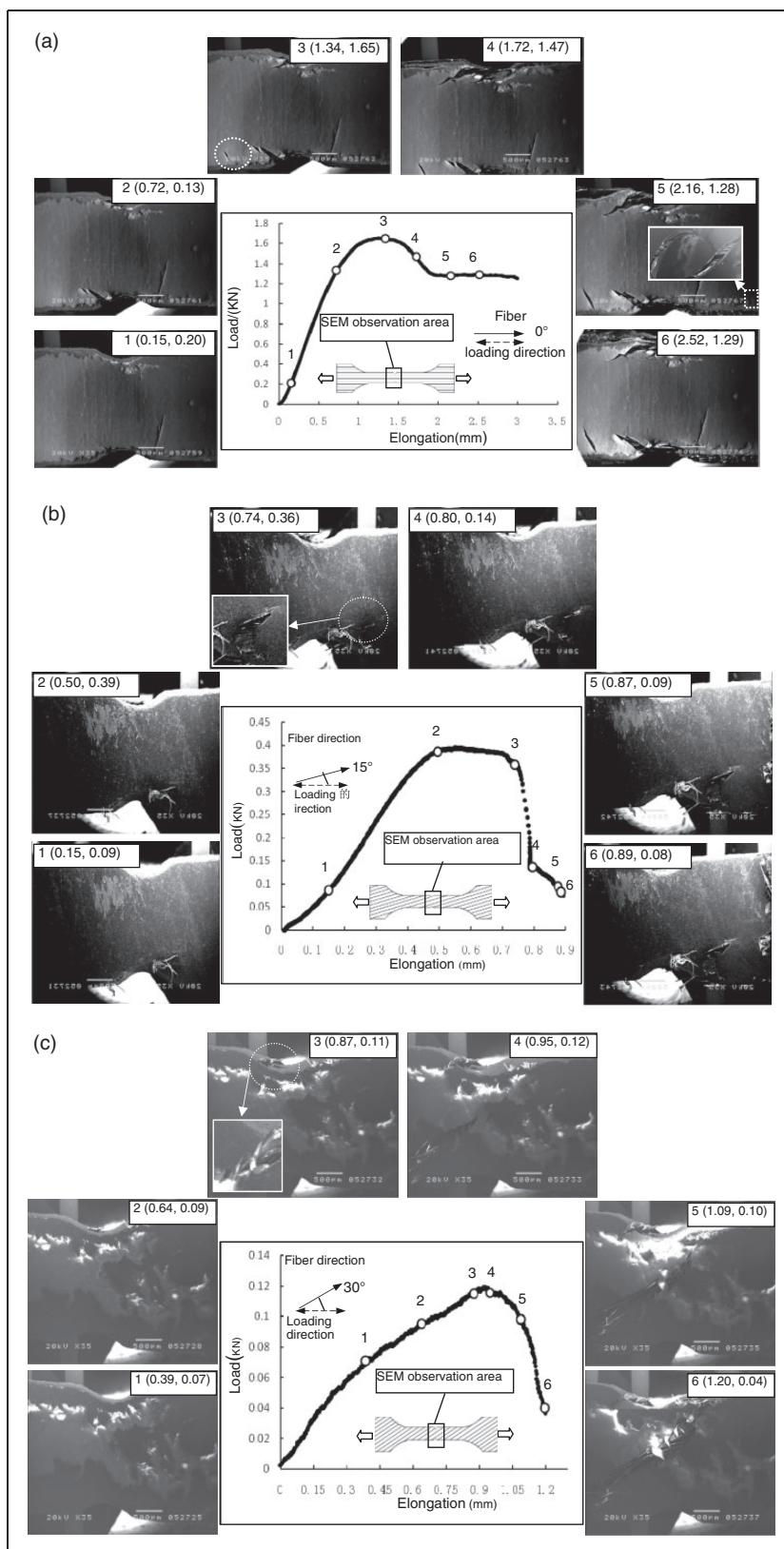
Figure 4. Load–deflection curves with micrographs of the observed microregion for the tensile deformation experiments of composites with different angles between the fiber and loading directions: (a) α = 0°, (b) α = 15°, (c) α = 30° (d) α = 45° and (e) α = 90°. Note: The numbers at the corner of the scanning electron microscopy photographs denote the photograph number and the corresponding load (kN) and deflection (mm).
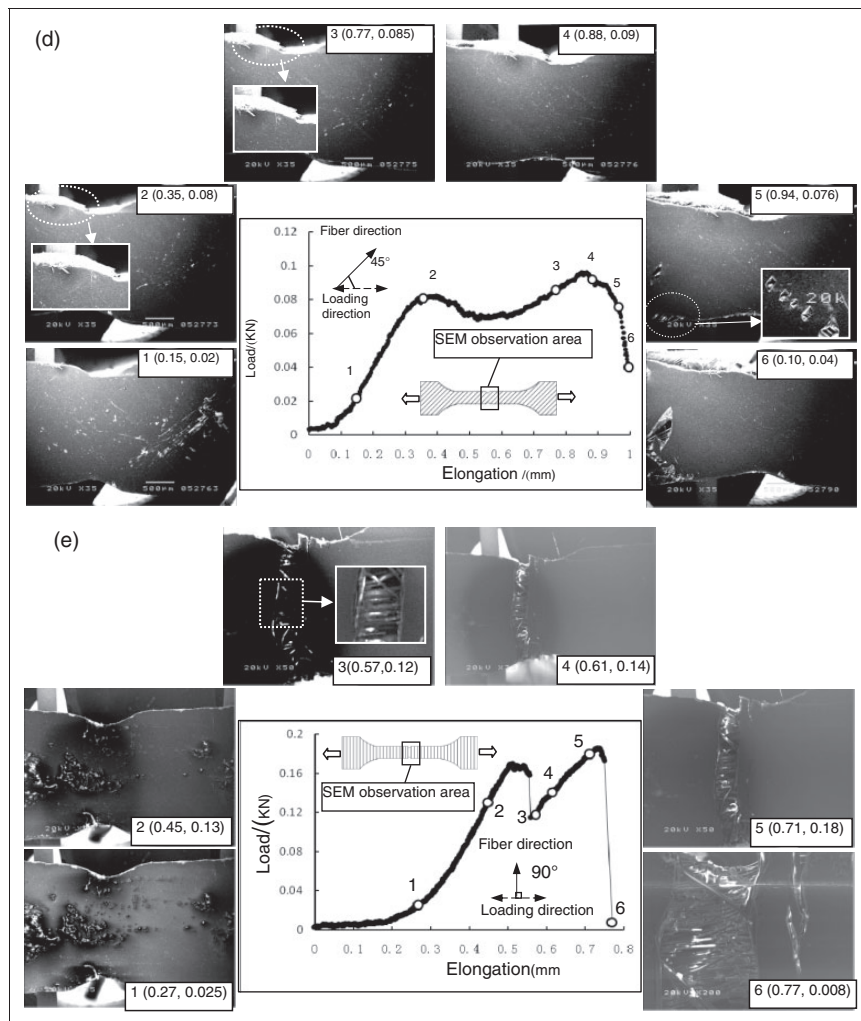
Figure 4. Continued.

Fatigue damage

In the following series of tests, we studied the fatigue damage evolution in the composites. Specimens with different fiber orientations were tested experimentally. The dimensions of the specimens are shown in Figure 7. The loading pattern was triangular wave loading and loading frequency was 10 Hz. Constant amplitude stress loading was applied, with the amplitude in the range of 0.2–0.6 KN (tension–tension cyclic loading), which is in elastic range of specimens. The loadings were carried out at room temperature (20°). The date was recorded by the system automatically for every 2×10^3 cycles. The loadings were continued up to 10^6 cycles if there was no obvious damage in observation.

Figures 8 and 9 present the micrographs showing the crack evolution formation in the composites. In samples with fiber angles below 30°, no fatigue failure was observed in the considered range of loading,

although a certain extent of shearing was seen in samples with angle of 30° (Figure 8(a)) after 10^6 cycles test. In specimens with angle between fibers and loading direction of 45° or more, the fatigue failure occurred (Figure 8(b)–(e)). Figure 8 shows the crack paths fluctuating between the directions of shear stresses, fiber directions and normal stresses. The shortest fatigue lifetime was for the composites with angle of 45°. The main damage mechanism was interface debonding and fatigue crack growth along the fiber interface (Figure 9).

Summarizing the results of the investigations, we can conclude that the damage mechanisms in GFRP composites strongly depend on the orientation and angle of the applied loading with the fiber direction. Matrix cracking was observed as the main damage mechanism for tensile axial (or slightly off-axis axial) loading; for all other cases (off-axis, tensile, compressive, cyclic tensile loadings), interface debonding and shear control were the damage mechanisms.
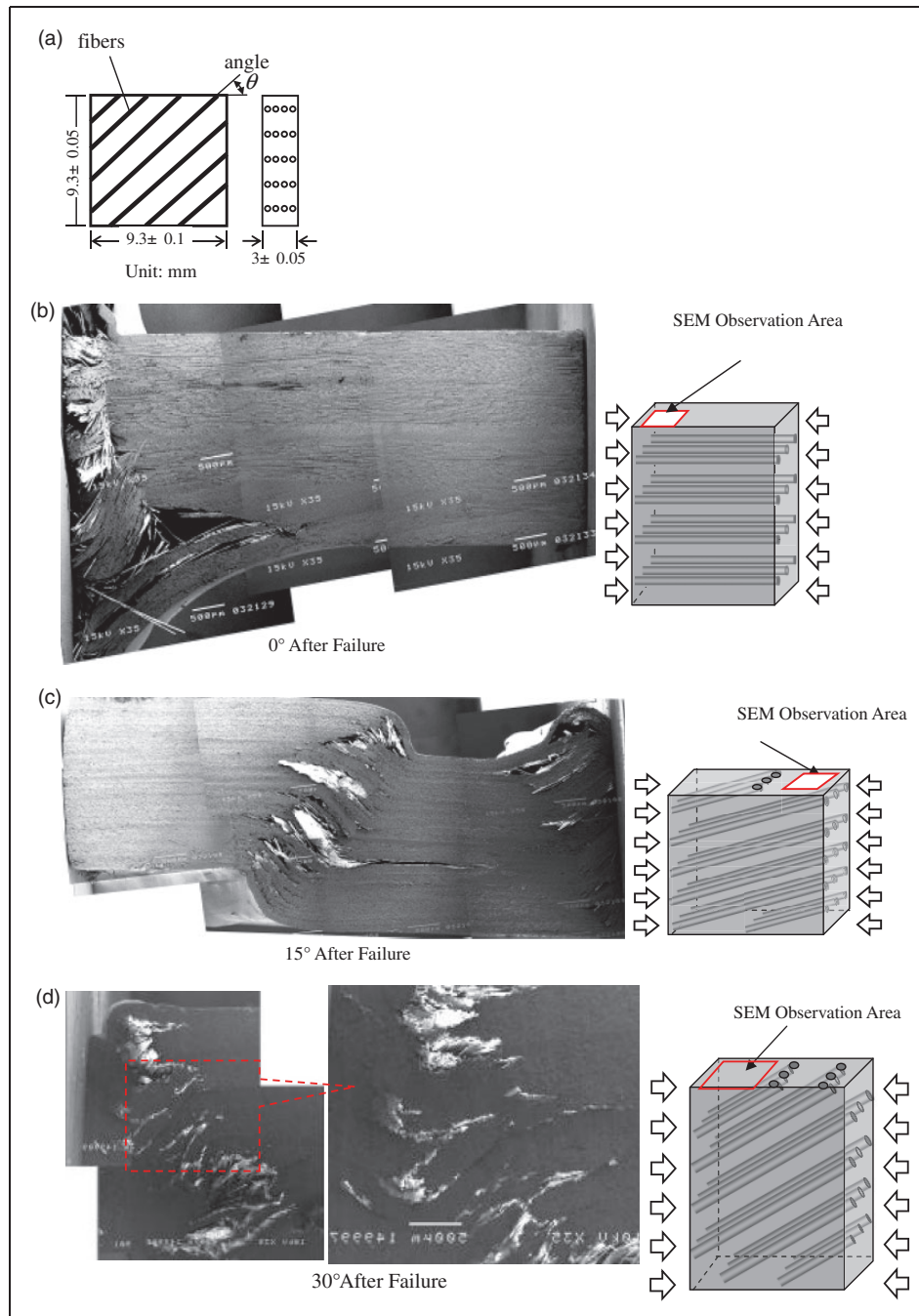
Figure 5. (a) Dimension of specimen for compression test and micrographs of the damage evolution for the compressive loading of composites with different angles between the fiber and loading directions: (b) 0°, (c) 15°, (d) 30°, (e) 60°, (f) 75° and (g) 90°.

Computational experiments: analysis of damage mechanisms of GFRP in three-dimensional computational models

Experimental testing of composites under various loading conditions is rather expensive in terms of labor and costs. The solution for this problem lies in the application of numerical experiments in which various materials (which are used or have a potential to be used for wind energy applications) are tested in computational models. In order to study the micromechanisms of damage evolution and effect of microscale parameters (fiber and matrix properties, interface strength, fiber misalignment, and so on) of composites on their strength, a series of special computational programs for
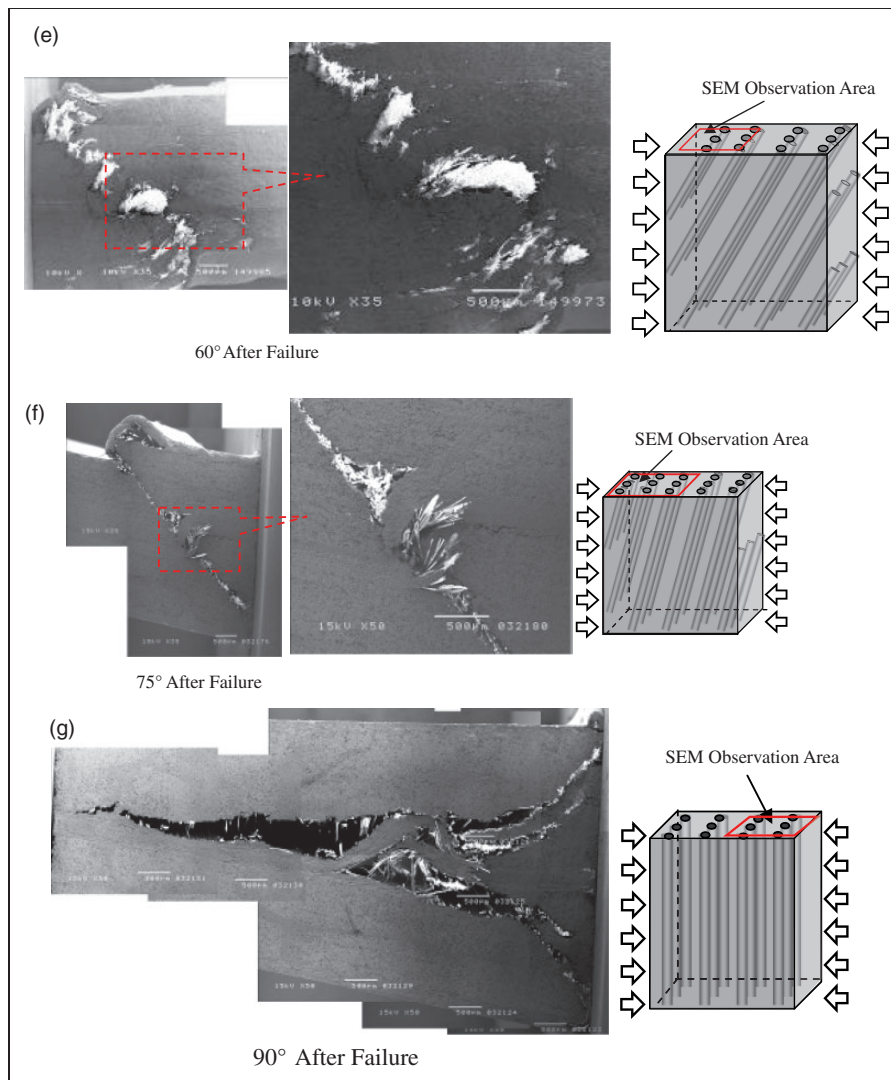
(e) 60° After Failure

(f) 75° After Failure

(g) 90° After Failure

Figure 5. Continued.

the automatic generation of three-dimensional (3D) computational micromechanical models of the composites has been developed and used in the numerical simulations[6–13] and Dai GM and Mishnaevsky Jr L. Fatigue of hybrid glass/carbon composites: computational studies (manuscript in preparation).

Damage mechanisms—interaction between matrix cracking and interface debonding: modeling results

In this section, we utilize the methods of computational micromechanics and damage mechanics to analyze the damage mechanisms in GFRP.

Using the software developed in previous studies,[6–10] we generated several multifiber unit cell models of composites. The finite element models of the unit cells were subject to a uniaxial tensile displacement loading. The dimensions of the unit cells were 10 mm in all three directions. A number of unit cells (with 15 fibers and 25% fiber volume content) were generated and subject to the mechanical loading.

The damage evolution was modeled using the ABAQUS subroutine user defined field. The glass fibers were considered as elastic isotropic solids, with Young's modulus of 72 GPa and Poisson's ratio of 0.26. The failure strength of glass fibers was assumed to be distributed by Weibull probability law

$$P(\text{Failure}) = 1 - \exp\left[-\left(\frac{\sigma}{\sigma_0}\right)^m\right] \quad (1)$$

with parameters $\sigma_0 = 1649$ MPa and $m = 3.09$. Here, σ indicates stress. The elastic properties of epoxy matrix were as follows. Young's modulus, 3790 MPa; Poisson's ratio, 0.37; bulk modulus, 5 GPa and
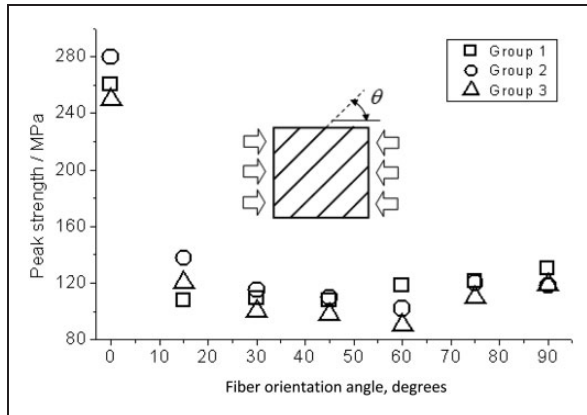
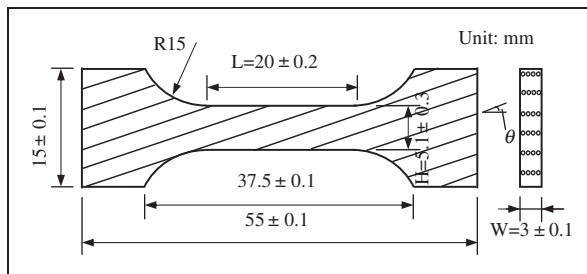**Figure 6.** Peak compressive strength versus fiber orientations.

Figure 7. Dimensions of specimen for fatigue tests.

instantaneous shear modulus, 1.38 GPa. The viscoelastic properties were described by single-term Prony series, with relaxation time 0.25 s and modulus ratio $g = 0.125$. The failure stress of epoxy matrix was 67 Mpa.[6] The thickness of the interface layer was 0.02 l; l indicates cell size. The interface layer was assumed to be a homogeneous isotropic material, with Young's modulus of 37.9 GPa (i.e. the average value of the Young's moduli of fiber and matrix materials) and Poisson's ratio of the matrix.

To simulate the interface damage, we used the "third phase" model of interface, which represents the interface as a thin layer of third phase between fibers and matrix.[6] More details are given elsewhere[6–15] and Dai GM and Mishnaevsky Jr L. Fatigue of hybrid glass/carbon composites: computational studies (manuscript in preparation).

First, we considered composites with strong, nondamageable interfaces. In order to evaluate the effect of matrix defects, we introduced the horizontal matrix cracks (1/6, 1/2 and 8/12 of the cell size, bridged by intact glass fibers). Figure 10 shows the maximal shear strain in the matrix with a long crack after the fiber failure. The stresses are very high in the bridging fibers and in the matrix regions between two neighboring fiber cracks. In the simulations, only a weak
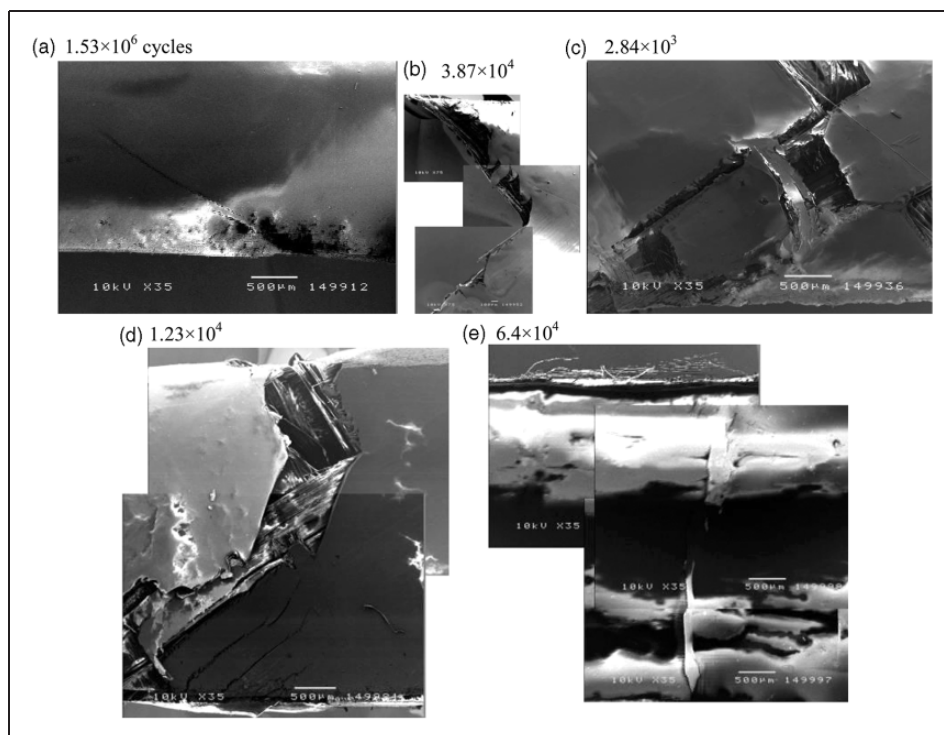

Figure 8. Micrographs of the damage evolution for the cyclic loading of composites with different angles between the fiber and loading directions: (a) 30°, (b) 45°, (c) 60°, (d) 75°, (e) 90°.

influence of the matrix cracks on the fiber fracture was observed.

In the next series of numerical experiments, we considered the interaction between the damage growth in the interface layer and the matrix defects. In a number of multifiber unit cells, each fiber was surrounded by intact, but damageable interface layers. Figure 11 shows the damage evolution in the fibers and matrix, observed in the simulations for the case of strong, intact matrix. One can see that the formation of the interfac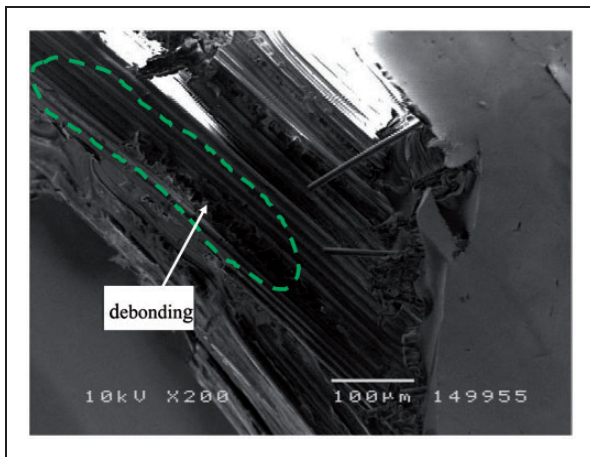e cracks takes place after the fiber cracking and in the vicinity of the fiber cracks. After an interface crack is formed, it can cause the formation of other interface cracks near neighboring fibers (in the case of relatively weak interfaces).

Furthermore, the simulations of the damage evolution in the unit cells with strong, nondamageable matrix and differently strong interface layers have been carried out. For the weak damageable interfaces, the interface damage begins the earlier the large rare matrix cracks. It was observed that the interface properties influence the sensitivity of the composites to the matrix defects: in the case of the weak fiber–matrix interface, the matrix defects can speed up the cracking in fibers and the composite failure.

Further simulations have been carried out for all three competing damage modes, in fiber, matrix and interface. Figure 12 shows the results of the simulations. The damage evolution begins by the formation of a crack in a fiber and (in another, rather far site) in the matrix ($\varepsilon = 0.01$). Then the interface crack forms nearby the fiber crack and the large matrix crack is formed ($\varepsilon = 0.015$).

In the case when all the three damage mechanisms are possible, the competition between the matrix cracking and the interface debonding is observed. In the area where the interface is damaged, no matrix crack forms; inversely, in the area, where the long matrix cracks are formed, the fiber cracking does not lead to interface damage.
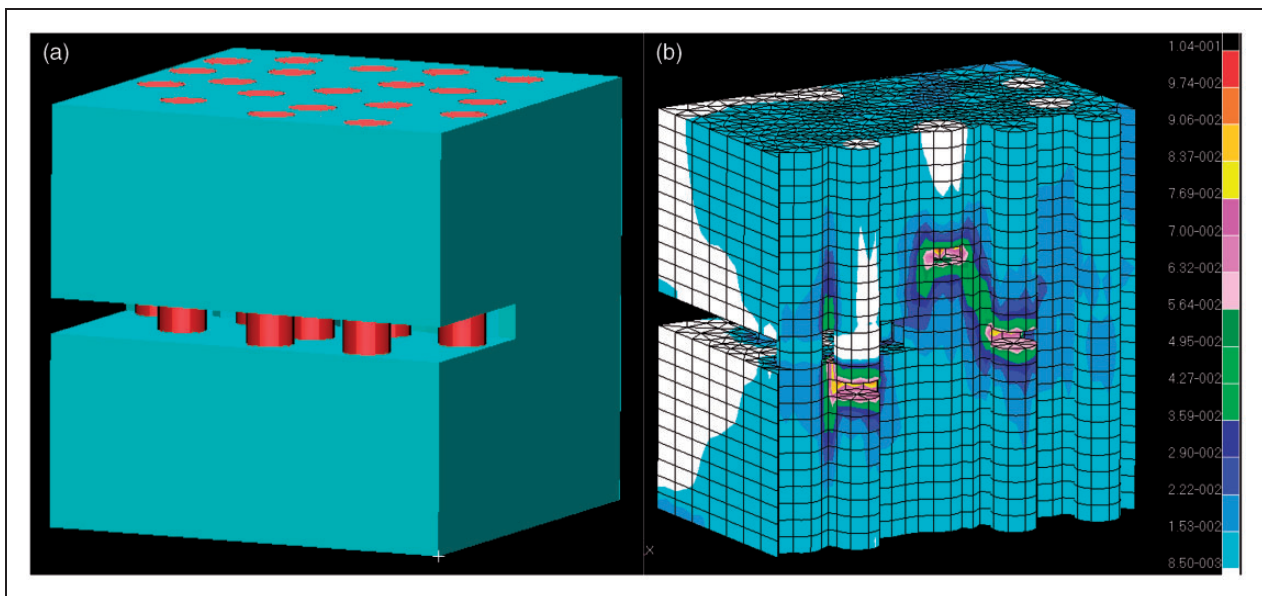

Figure 9. Interfacial debonding along fiber orientation in sample with fiber orientation of 45°.

Figure 10. (a) Multifiber unit cell model of composite and (b) maximal shear strain distribution in the matrix with the long matrix crack. Reprinted from the study of Mishnaevsky Jr and Brøndsted,[6] with kind permission from Elsevier.
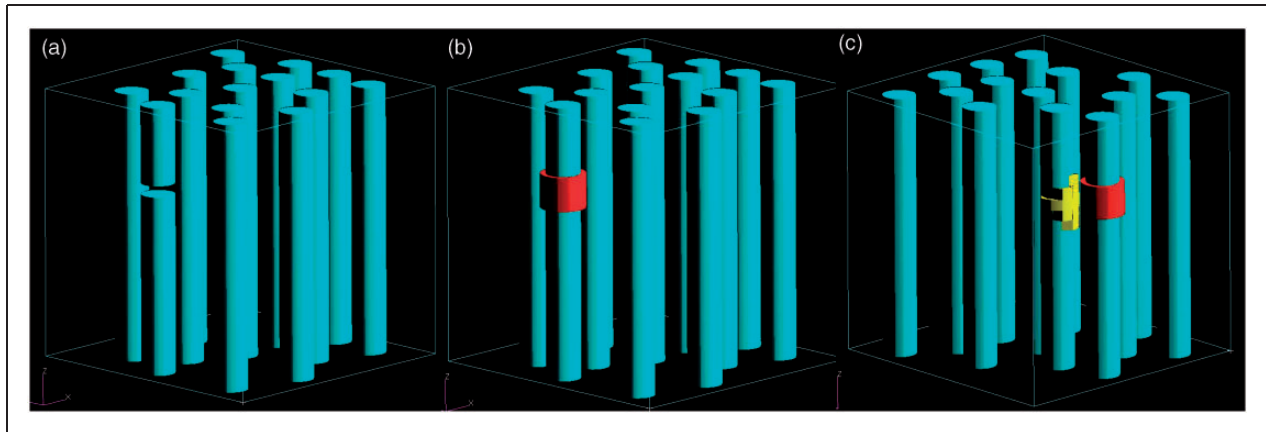
Figure 11. Damage evolution in a composite with damageable interface and fibers and strong matrix: (a) fiber cracking, $\varepsilon = 0.007$, ε indicates applied strain, (b) interface damage near the fiber crack, $\varepsilon = 0.0072$, (c) interface damage near the neighboring fiber, $\varepsilon = 0.0095$.
Reprinted from the study of Mishnaevsky Jr and Brøndsted,6 with kind permission from Elsevier.
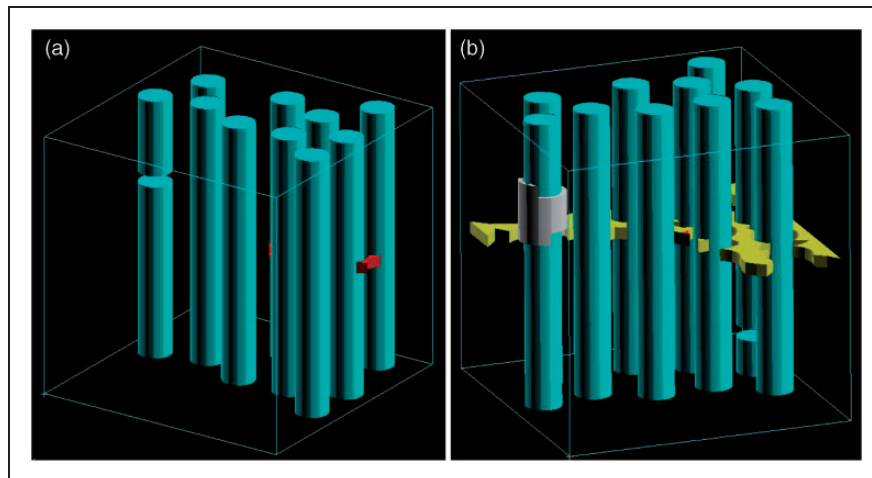

Figure 12. Competition of damage modes: (a) one failed fiber and a few microcracks in the matrix (red), $\varepsilon = 0.01$, and (b) two fibers have failed, the interface crack is formed in the vicinity of a fiber crack and the matrix crack is formed ($\varepsilon = 0.015$). Reprinted from the study of Mishnaevsky Jr and Brøndsted,[6] with kind permission of Elsevier.

Compression damage in GFRP: modeling results

In further computational experiments[12,16] (also Dai GM and Mishnaevsky Jr L. Fatigue of hybrid glass/carbon composites: computational studies, manuscript in preparation), we studied the damage mechanisms of glass fiber–epoxy composites under compressive loading.

We considered the unit cells with many fibers and various angles between the loading vector and fibers (30°, 50°, 70° and 90°).

To model the material degradation, we decided to use eXtended finite element method (XFEM) (see the study by Mishnaevsky Jr et al.[15]) instead of damage mechanics-based user defined field subroutine. This approach allows us to include also fracture toughness criteria under mode II and mode III fracture. The virtual crack closure technique is used here to calculate the strain energy release rates. The size of unit cells was $70 \times 70 \times 92\,\mu m$. The glass fiber has a radius of $8\,\mu m$ while the interface layer has a thickness of $0.8\,\mu m$. The C3D8R element (a 3D eight-node linear brick) and a reduced integration element in conjunction with C3D4 (a 3D four-node linear tetrahedron element) were used in the FE analysis. A total of 22,968 elements and 28,262 elements are used in the aligned and misaligned models. Compressive strengths of the glass fibers and of matrix were taken at 1500 and 88 MPa, respectively. The crack growth analysis is based on the linear elastic fracture mechanics approach.
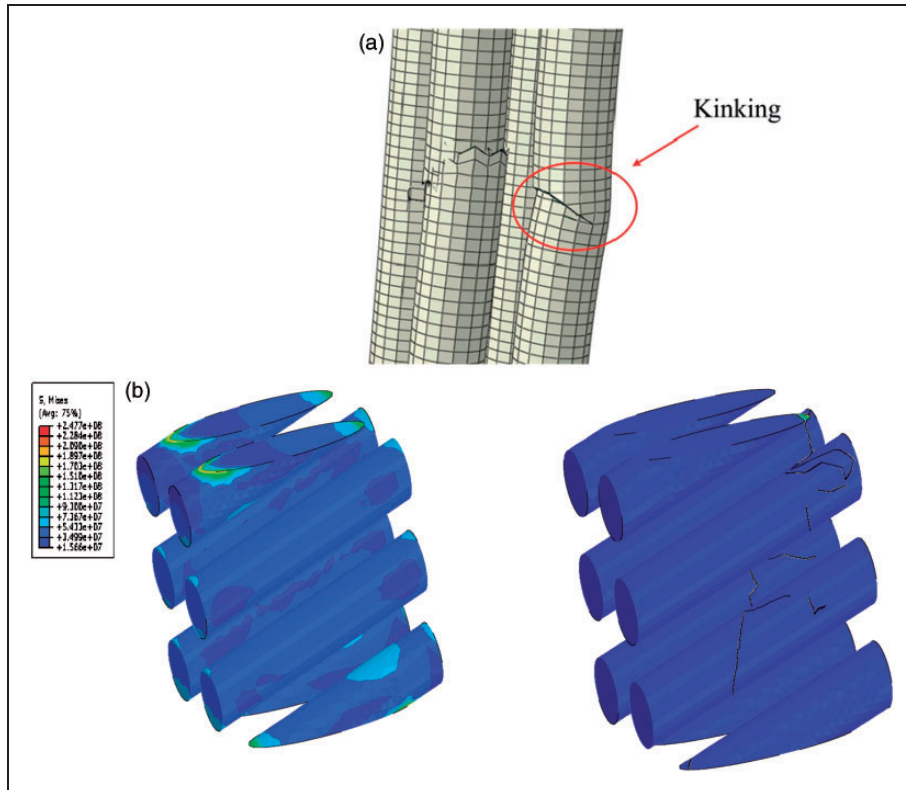
Figure 13. Damage mechanisms in composites: (a) kinking in a composite with randomly misaligned fibers and (b) cracking in a composite with 70° inclined fibers.
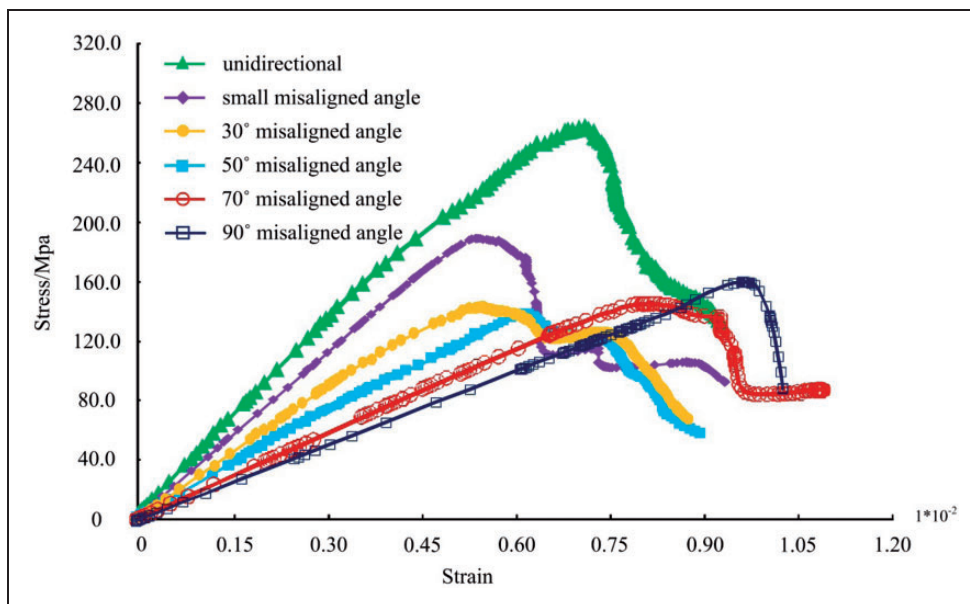

Figure 14. Strain–stress curves for glass fiber-reinforced composite with randomly misaligned (0–10°) and inclined fibers (30°, 50° and 70°) under compression loading. Reprinted from the study of Zhou et al.,[12] with kind permission from Elsevier.
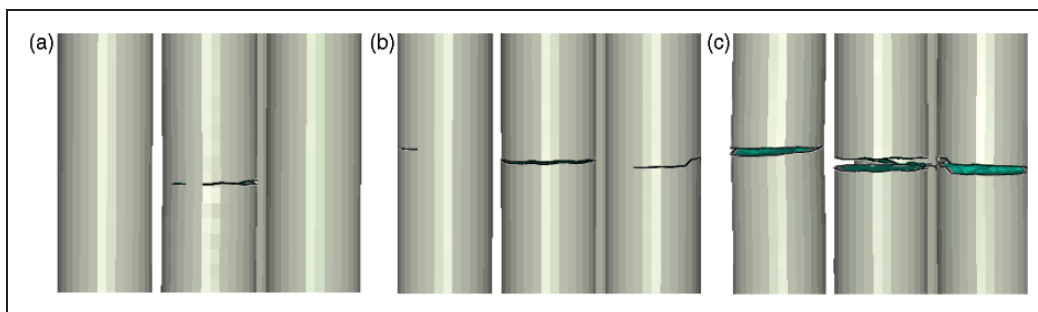
Figure 15. Damage evolution in fibers under cyclic (tensile–tensile) loading: (a) crack initiation in a fiber and first fiber failure, (b) failure of second, neighboring fiber and (c) third fiber failure.
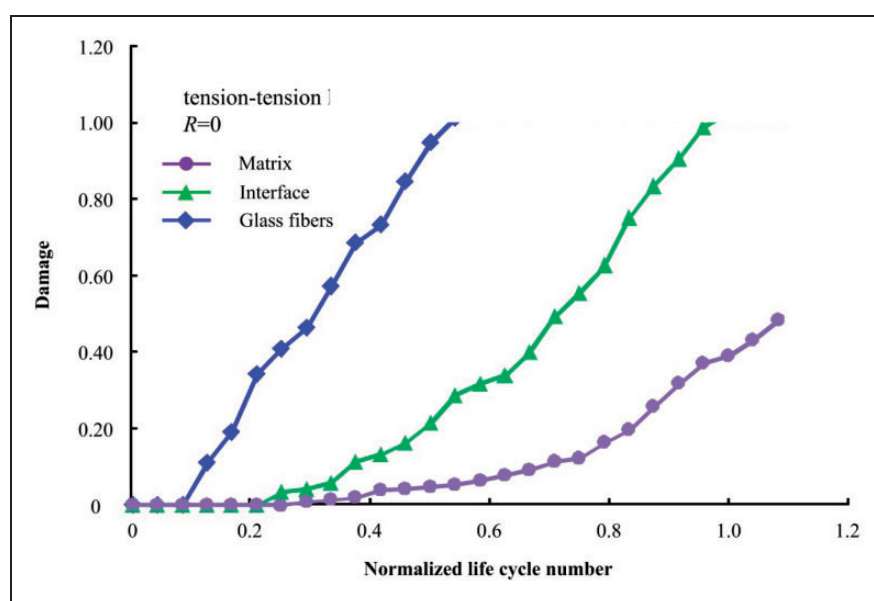

Figure 16. Damage parameters evolution of different materials phases (the cycle numbers are normalized by the number when all the interface are damaged, in this case 2.1×10^6 cycles).

Figure 13(a) shows the glass fiber kinking in the unit cell with vertical fibers observed in the numerical simulations (compare with 'Compression loading', where the fiber kinking was also observed, experimentally).

Figure 13(b) shows the crack path in an inclined glass fiber (70°) and the stress distribution (at the crack initiation). One can see that in the case of the off-axis loading, the cracks fluctuate, propagating both through the fiber in the direction of loading and along the fiber length. The fiber splitting as well as shear controlled cracks and crack deviations are observed.

Figure 14 shows the stress–strain curves for the several simulated unit cells.[12] Comparing the numerical results with the experimental ones (Figure 6), we can see that the results of the numerical experiments

correspond with the results of the experimental observations. The peak stress for the case of vertical loading (i.e. along the fiber axis) is reduced by about two times when the angle between the fibers and loading reaches 30–50° and slightly increases for the angles 70–90°.[12]

Modeling of fatigue cracking in GFRP

Furthermore, a series of numerical simulations of damage evolution in composites under cyclic tensile–tensile loading has been carried out (Dai GM and Mishnaevsky Jr L. Fatigue of hybrid glass/carbon composites: computational studies, manuscript in preparation). Figure 15 shows the crack initiation and growth in fibers. Figure 16 shows the damage curves, i.e. the damage parameters calculated separately for the fibers, interface layer and matrix plotted versus the

normalized loading cycle number. (The damage parameter was calculated as the horizontal projection of the crack in a given phase divided by the total area of the projection of the phase.)

From Figure 16, it can be seen that the damage evolution under tension–tension cyclic loading begins first in fibers. Much later, the interface damage starts and after some time, it leads to matrix cracking. This also explains the high lifetime observed under axial tension–tension cyclic loadings. Since the fatigue lifetime in the case of small angles between fibers and loadings is controlled by fiber strength, this becomes much higher than when the loadings are applied at an angle of 30° or more to the fibers (in this case, interface damage mechanisms take over the control of the fatigue lifetime).

Summarizing the observations from the experiments and numerical studies, one can conclude that while the strength and reliability of fiber-reinforced composites under tensile axial loading is controlled mainly by fiber strength, in almost all other cases (compression, off-axis tension and fatigue), the interface strength and interface shear properties play key roles in determining composite strength. This is an important result for the development and design of wind turbine blade materials. As noted in 'Introduction', wind blade materials are subject to complex multiaxial loading, including compressive (downwind side) and tensile (upwind side) randomly varying stresses. From the above results, we can see that the most important factor for the improvement of materials used to manufacture wind turbine (and, ultimately, to improve the reliability of wind turbines) is to achieve control of interface properties of composites, which can be accomplished by using sized fibers, or nanoengineering of interfaces.

Conclusions

In this article, an overview of research investigations on the experimental and numerical analyses of microscale damage mechanisms in glass fiber-reinforced polymers, carried out in collaboration between several Chinese and Danish teams, is provided. Keeping in mind the potential applications of the materials for wind energy applications (first of all, wind blades), we paid special attention to the effect of the off-axis, compressive and cyclic loading effects on the damage mechanisms of composites.

With a knowledge of the damage mechanisms responsible for the degradation and failure of wind turbine materials under service conditions, we searched for ways and methods to control these mechanisms, thereby increasing the lifetime and reliability of wind blades.

From a series of experimental (SEM in situ experiments, three-point bending, tension, compression, fatigue) and numerical studies (3D FE computational experiments), we have clarified some most typical damage mechanisms in wind energy composites.

In particular, we demonstrated that the damage mechanisms in GFRP composites strongly depend on the orientation of fibers and on the angle between applied loading and the fiber direction.

Matrix cracking was observed to be the main damage mechanism for tensile axial (or almost axial) loading; for all other cases (off-axis tensile, compressive, cyclic tensile loadings), interface debonding and shear controlled damage are the most important damage mechanisms. The interface defects and generally the interface damage evolution play the role of a competitor for the matrix and fiber cracking damage mechanisms under tensile loading. However, as long as the interface is strong and damage free, the composite can sustain rather high level of matrix defects without the fiber cracking.

For the compressive loading of aligned or even slightly misaligned fiber composites, the main damage mechanism is fiber kinking. In the case of the inclined fibers, the damage mechanism changes—no more kinking but rather fiber cracking, with the crack propagating along the loading direction, partially shear (mode II) controlled.

Under axial cyclic tension–tension loading, the fatigue lifetime in the case of small angles between fibers and loadings is controlled by the fiber strength and is therefore very high. Under off-axis cyclic loading (when the loadings are applied at angle of 30° or more to the fibers), interface damage mechanisms are controlling the fatigue lifetime and lead to much shorter lifetime.

Conflict of interest

None declared.

References

1. Brøndsted P, Lilholt H and Lystrup A. Composite materials for wind power turbine blades. *Ann Rev Mater Res* 2005; 35: 505–538.

2. Mishnaevsky L Jr, Brøndsted P, Nijssen R, et al. Materials of large wind turbine blades: recent results in testing and modelling. *Wind Energy* 2012; 15(1): 83–97.

3. Mohamed MH and Wetzel KK. 3D woven carbon/glass hybrid spar cap for wind turbine rotor blade. *Trans ASME J Solar Energy Eng* 2006; 128: 562–573.

4. Thomsen OT. Sandwich materials for wind turbine blades - present and future. *J Sandwich Struct Mater* 2009; 11(1): 7–26.

5. Zhou HW, Mishnaevsky L Jr, Brøndsted P, et al. SEM in situ laboratory investigations on damage growth in GFRP composite under three-point bending tests. *Chinese Sci Bull* 2010; 55(12): 1199−1208.

6. Mishnaevsky L Jr and Brøndsted P. Micromechanisms of damage in unidirectional fiber reinforced composites: 3D computational analysis. *Compos Sci Technol* 2009; 69(7–8): 1036–1044.

7. Mishnaevsky L Jr and Brøndsted P. Three-dimensional numerical modelling of damage initiation in UD fiber-reinforced composites with ductile matrix. *Mater Sci Eng A* 2008; 498(1-2): 81–86.

8. Mishnaevsky L Jr and Brøndsted P. Micromechanical modeling of damage and fracture of unidirectional fiber reinforced composites: a review. *Comput Mater Sci* 2009; 44(4): 1351–1359.

9. Wang HW, Zhou HW, Mishnaevsky L Jr, et al. Single fibre and multifibre unit cell analysis of strength and cracking of unidirectional composites. *Comput Mater Sci* 2009; 46(4): 810–820.

10. Dai GM and Mishnaevsky L Jr. Damage evolution in nanoclay-reinforced polymers: a three-dimensional computational study. *Compos Sci Technol* 2013; 74: 67–77.

11. Wang HW, Zhou HW, Peng RD, et al. Nanoreinforced polymer composites: 3D FEM modeling with effective interface concept. *Compos Sci Technol* 2011; 71(7): 980–988.

12. Zhou HW, Yi HY, Gui LL, et al. Compressive damage mechanism of GFRP composites under off-axis loading: experimental and numerical investigations. *Compos Part B* 2013; 55: 119–127.

13. Qing H and Mishnaevsky L Jr. Unidirectional high fiber content composites: automatic 3D FE model generation and damage simulation. *Comput Mater Sci* 2009; 47(2): 548–555.

14. Mishnaevsky L Jr, Lippmann N and Schmauder S. Computational modeling of crack propagation in real microstructures of steels and virtual testing of artificially designed materials. *Int J Fract* 2003; 120(4): 581–600.

15. Mishnaevsky L Jr. Functionally gradient metal matrix composites: numerical analysis of the microstructure-strength relationships. *Compos Sci Technol* 2006; 66(11-12): 1873–1887.

16. Mishnaevsky L Jr and Brøndsted P. Statistical modelling of compression and fatigue damage of unidirectional fiber reinforced composites. *Compos Sci Technol* 2009; 69(3-4): 477–484.